Inorganic Chemistry
Article

Inorg. Chem. **2009**, *48*, 9419–9426 **9419**
DOI: 10.1021/ic9012697

A New Tripodal Ligand System with Steric and Electronic Modularity for Uranium Coordination Chemistry

Suzanne C. Bart, Frank W. Heinemann, Christian Anthon, Christina Hauser, and Karsten Meyer*

Department of Chemistry and Pharmacy, Inorganic Chemistry, Friedrich-Alexander University of Erlangen-Nuremberg, Egerlandstrasse 1, 91058 Erlangen, Germany

Received July 2, 2009

The synthesis of a potentially redox active tripodal ligand containing a tris(aryloxide) functionalized mesitylene anchor, (($^{t\text{Bu}}$ArOH)$_3$mes) (**1**), and its metalation with low-valent uranium to form [(($^{t\text{Bu}}$ArO)$_3$mes)U] (**1-U**) is reported. The results from characterization by X-ray crystallography, spectroscopic studies, and computational analysis, as well as initial reactivity studies, support a +3 uranium oxidation state. Comparison to the previously synthesized complex, [(($^{t\text{Bu}}$ArO)$_3$tacn)U] (**2-U**), featuring the redox-innocent triazacyclononane anchor reveals that changing the anchor from the flexible triazacyclononane to a rigid mesityl fragment increases the structural flexibility of the aryloxide substituents in complexes of **1**. The synthesis and crystal structures of uranium(IV) amide complexes of **1-U** and **2-U** are discussed.

Introduction

It is well established that the electronic and structural architecture of ancillary ligands largely controls the reactivity of metal coordination complexes. This has also been proven for the coordination chemistry of actinide complexes, which because of the accessibility of uranium starting materials is dominated by reports of uranium based complexes.[1a−c] Despite the vast amount of research reported on uranium coordination chemistry supported by ancillary ligands, very few uranium complexes have been synthesized containing redox-active ligands.[1d,2a−2d] More recently, Arnold and Diaconescu have introduced the potentially redox-active ferrocene diamide ligand system to the revitalized coordination chemistry of uranium.[2e−g] Such so-called "non-innocent" ligands have been widely used in transition metal chemistry and are attractive because of their ability to support complexes in unusual electronic states,[5−9] thus mediating small molecule activation and industrially relevant chemical transformations.[3,4] Often these processes are performed by molecules in low-valent oxidation states, and many have been produced by sterically induced reduction.[2h−o] The arene-bridged dinuclear uranium complex, [{(Ar[R]N)$_2$U}$_2$(μ-C$_7$H$_8$)] (R = ^{t}Bu, Ar = 3,5-C$_6$H$_3$Me$_2$), synthesized by Cummins and co-workers, illustrates well the principles behind redox-active ligand coordination.[10,11]

*To whom correspondence should be addressed. E-mail: kmeyer@chemie.uni-erlangen.de.

(1) (a) Ephritikhine, M. *Dalton Trans.* **2006**, 2501. (b) Evans, W. J.; Kozimor, S. A. *Coord. Chem. Rev.* **2006**, *250*(7−8), 911. (c) Sessler, J. L.; Melfi, P. J.; Pantos, G. D. *Coord. Chem. Rev.* **2006**, *250*(7−8), 816. (d) Danopoulos, A. A.; Hankin, D. M.; Cafferkey, S. M.; Hursthouse, M. B. *Dalton Trans.* **2000**, 1613.

(2) (a) Arliguie, T.; Doux, M.; Mezailles, N.; Thuery, P.; Le Floch, P.; Ephritikhine, M. *Inorg. Chem.* **2006**, *45*, 9907. (b) Mehdoui, T.; Berthet, J.-C.; Thuery, P.; Salmon, L.; Riviere, E.; Ephritikhine, M. *Chem.—Eur. J.* **2005**, *11*, 6994. (c) Del Piero, G.; Perego, G.; Zazzetta, A.; Brandi, G. *Cryst. Struct. Commun.* **1975**, *4*, 521. (d) Herzog, S.; Oberender, H. *Z. Chem.* **1963**, *3*, 429. (e) Wiley, R. O.; Von Dreele, R. M.; Brown, T. M. *Inorg. Chem.* **1980**, *19*, pp 3351. (f) Monreal, M. J.; Diaconescu, P. L. *Organometallics* **2008**, *27*, 1702. (g) Westmoreland, I.; Arnold, J. *Acta Crystallogr., Sect. E: Struct. Rep. Online* **2006**, *E62*, m2303. (h) Monreal, M. J.; Carver, C. T.; Diaconescu, P. L. *Inorg. Chem.* **2007**, *46*, 7226. (i) Evans, W. J.; Takase, M. K.; Ziller, J. W.; DiPasquale, A. G.; Rheingold, A. L. *Organometallics* **2009**, *28*, 236. (j) Evans, W. J.; Walensky, J. R.; Furche, F.; Ziller, J. W.; DiPasquale, A. G.; Rheingold, A. L. *Inorg. Chem.* **2008**, *47*, 10169. (k) Evans, W. J.; Montalvo, E.; Kozimor, S. A.; Miller, K. A. *J. Am. Chem. Soc.* **2008**, *130*, 12258. (l) Evans, W. J.; Miller, K. A.; Ziller, J. W. *Angew. Chem., Int. Ed.* **2008**, *47*, 589. (m) Evans, W. J.; Miller, K. A.; Hillman, W. R.; Ziller, J. W. *J. Organomet. Chem.* **2007**, *692*, 3649. (n) Evans, W. J.; Miller, K. A.; Kozimor, S. A.; Ziller, J. W.; DiPasquale, A. G.; Rheingold, A. L. *Organometallics* **2007**, *26*, 3568. (o) Evans, W. J.; Kozimor, S. A. *Coord. Chem. Rev.* **2006**, *250*, 911. (p) Evans, W. J.; Kozimor, S. A.; Ziller, J. W. *Chem. Commun.* **2005**, 4681.

(3) Bart, S. C.; Lobkovsky, E.; Chirik, P. J. *J. Am. Chem. Soc.* **2004**, *126*, 13794.

(4) Ringenberg, M. R.; Kokatam, S. L.; Heiden, Z. M.; Rauchfuss, T. B. *J. Am. Chem. Soc.* **2008**, *130*, 788.

(5) Bart, S. C.; Lobkovsky, E.; Bill, E.; Wieghardt, K.; Chirik, P. J. *Inorg. Chem.* **2007**, *46*, 7055.

(6) Bart, S. C.; Chlopek, K.; Bill, E.; Bouwkamp, M. W.; Lobkovsky, E.; Neese, F.; Wieghardt, K.; Chirik, P. J. *J. Am. Chem. Soc.* **2006**, *128*, 13901.

(7) Khusniyarov, M. M.; Hamrms, K.; Burghaus, O.; Sundermeyer, J.; Sarkar, B.; Kaim, W.; van Slageren, J.; Duboc, C.; Fiedler, J. *Dalton Trans.* **2008**, 1355.

(8) Maurer, J.; Linseis, M.; Sarkar, B.; Schwederski, B.; Niemeyer, M.; Kaim, W.; Zalis, S.; Anson, C.; Zabel, M.; Winter, R. F. *J. Am. Chem. Soc.* **2008**, *130*, 259.

(9) Ray, K.; Petrenko, T.; Wieghardt, K.; Neese, F. *Dalton Trans.* **2007**, 1552.

(10) Diaconescu, P. L.; Cummins, C. C. *J. Am. Chem. Soc.* **2002**, *124*, 7660.

(11) (a) Diaconescu, P. L.; Arnold, P. L.; Baker, T. A.; Mindiola, D. J.; Cummins, C. C. *J. Am. Chem. Soc.* **2000**, *122*, 6108. (b) Evans, W. J.; Kozimor, S. A.; Ziller, J. W.; Kaltsoyannis, N. *J. Am. Chem. Soc.* **2004**, *126*, 14533.

Published on Web 09/09/2009

Scheme 1. Synthesis of [(($^{t\,Bu}$ArO)$_3$mes)U] (**1-U**)

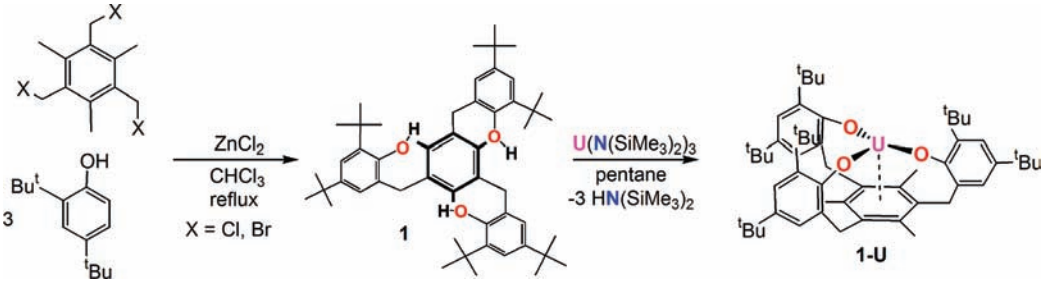

Although spectroscopically the complex [{(Ar[R]N)$_2$U}$_2$-(μ-C$_7$H$_8$)] appears to contain two U(III) centers, reactivity studies have demonstrated that it behaves as expected for two divalent uranium ions. After initial extrusion of the bridging toluene, it acts as a four-electron reductant toward small molecules. Two δ symmetry backbonds, one from each of the uranium centers to the arene, are believed to allow the uranium to access its formal low-valent +2 state. Similarly the bridging arene complex, [{(C$_5$Me$_5$)$_2$U}$_2$(μ:η^6-η^6-C$_6$H$_6$)], acts as a six electron reductant.[11b] Inspired by these report as well as others demonstrating the drastic impact of small alterations in ligand architecture,[12−15] we sought to utilize a similar methodology for the activation of small molecules by incorporating an arene ring as part of a potentially redox-active chelating ligand for uranium and other large metal ions.

Previously, we have focused on small molecule activation chemistry at low- and high-valent uranium complexes supported by aryloxide substituted triazacyclononane ligands, as in [((^{R}ArO$_3$)tacn)U^{III}] and [((^{R}ArO$_3$)tacn)U^V(NSiMe$_3$)] (R = ^{t}Bu, Ad).[16,17] Since these complexes feature a redox-innocent tris(aryloxide) polyamine chelator, a useful comparison of the reactivity and the electronic structure of complexes containing a newly developed ligand with an arene anchor can be made. For the development of versatile uranium coordination chemistry, the new ligand framework should be readily synthesized and modified, allowing for the possibility to vary the molecular and electronic architecture to direct complex reactivity. On the basis of a modular approach, we designed a tripodal ligand framework, comprising a mesitylene anchor and coordinating aryloxide pendant arms, which exhibits the above traits. The anchor and aryloxide pendant arms can be modified by selecting different arene and phenol derivatives. The arene framework could potentially serve as an electron source/sink, and provides the ability for δ backbonding interactions between the uranium f orbitals and the 2-fold degenerate empty arene π* orbitals, similar to that observed in [{(Ar[R]N)$_2$U}$_2$-(μ-C$_7$H$_8$)] and [{(C$_5$H$_5$)$_2$U}$_2$(μ:η_6,η_6-C$_6$H$_6$)]. Herein, the synthesis of this novel arene-based ligand system and the metalation with uranium will be reported. The molecular and electronic structures of the resulting complexes along with their reactivity are discussed and compared to the analogous complexes of the triazacyclononane anchored ligand system.

Results and Discussion

The tripodal ligand 1,3,5-trimethyl-2,4,6-tris(2,4-di-*tert*-butyl phenol)methyl)benzene, ($^{t\,Bu}$ArOH$_3$)mes (**1**), was synthesized by refluxing a solution of 2,4,6-tris(halomethyl)-mesitylene (halo = chloro,[18a] bromo[18b]) with 3 equiv of commercially available 2,4-di-*tert*-butyl phenol and 0.5 equiv of ZnCl$_2$ in CHCl$_3$ (Scheme 1). This procedure afforded the desired ligand as an analytically pure solid after recrystallization.[18c] Analysis by ^{1}H NMR spectroscopy (C$_6$D$_6$) showed the seven expected peaks for **1**, including resonances for the *tert*-butyl groups at 1.09 and 1.34 ppm, and a resonance for the mesitylene methyl groups at 2.10 ppm. The benzylic protons appear as a singlet at 3.94 ppm, while two aromatic protons appear as doublets at 7.07 and 6.63 ppm (J = 2.34 Hz).

Crystals of **1** suitable for X-ray diffraction were grown from a mixture of acetonitrile, water, and hydrochloric acid. The results confirmed formation of the desired ligand, ($^{t\,Bu}$ArOH)$_3$mes. The molecular structure (Figure 1) shows the central mesitylene anchor with three aryloxide arms, pointing away from each other to avoid unfavorable steric interactions. The C−C bond distances of the mesitylene anchor average to 1.41 Å (Table 1) and are the same within error as those in 2,4,6-tris(chloromethyl)mesitylene (see Supporting Information for complete list).

Addition of a pentane solution of [U(N(SiMe$_3$)$_2$)$_3$][33] to a stirring solution of the free ligand, ($^{t\,Bu}$ArOH$_3$)mes (**1**), resulted in clean metalation of the ligand with extrusion of 3 equiv of hexamethyldisilazane (Scheme 1). Filtration followed by removal of the volatiles produced a dark purple solid assigned as [(($^{t\,Bu}$ArO)$_3$mes)U] (**1-U**) in accordance with combustion analysis. The ^{1}H NMR spectrum for **1-U** displays the six expected peaks (Figure 2). The resonances for the *tert*-butyl groups are paramagnetically shifted and broadened from those of the free ligand to −0.85 and 2.03 ppm. The benzylic protons in **1-U** are equivalent, and shifted upfield from their diamagnetic reference values to −22.87 ppm, while the protons for the mesitylene methyl groups appear strongly shifted at −38.61 ppm. In contrast, the protons on the aryloxide rings are shifted little from those of the free ligand. The observation of equivalent benzylic protons in **1-U** is notably different from the tacn-based system, [(($^{t\,Bu}$ArO)$_3$-tacn)U], where the benzylic (and triazacyclononane) protons appear diastereotopic.

(12) Castro-Rodriguez, I.; Meyer, K. *J. Am. Chem. Soc.* **2005**, *127*, 11242.
(13) Castro-Rodriguez, I.; Nakai, H.; Zakharov, L. N.; Rheingold, A. L.; Meyer, K. *Science* **2004**, *305*, 1757.
(14) Summerscales, O. T.; Cloke, F. G. N.; Hitchcock, P. B.; Green, J. C.; Hazari, N. *J. Am. Chem. Soc.* **2006**, *128*, 9602.
(15) Summerscales, O. T.; Cloke, F. G. N.; Hitchcock, P. B.; Green, J. C.; Hazari, N. *Science* **2006**, *311*, 829.
(16) Castro-Rodriguez, I.; Olsen, K.; Gantzel, P.; Meyer, K. *J. Am. Chem. Soc.* **2003**, *125*, 4565.
(17) Castro-Rodriguez, I.; Olsen, K.; Gantzel, P.; Meyer, K. *Chem. Commun.* **2002**, 2764.
(18) (a) Tveten, J. L. U.S. Patent 3336402, **1967**. (b) Van der Made, A. W.; Van der Made, R. H. *J. Org. Chem.* **1993**, *58*, 1262. (c) Kochansky, J.; Cohen, C. F.; Lusby, W. R. *J. Agric. Food Chem.* **1995**, *43*, 2974.

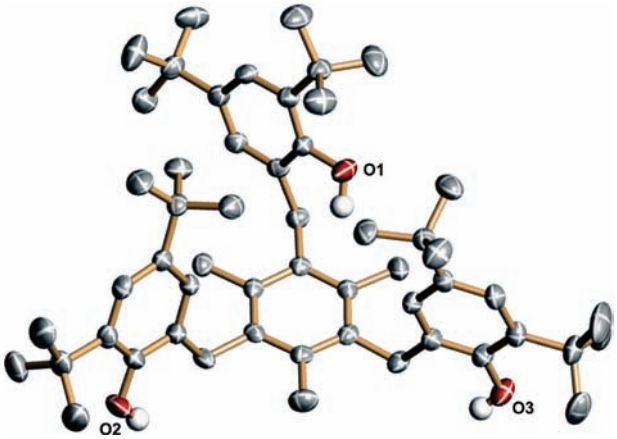

Figure 1. Molecular structure of ($^{t\,Bu}$ArOH$_3$)mes (**1**) in crystals of (**1**·CH$_3$CN). Selected hydrogen atoms and co-crystallized solvent molecules have been omitted for clarity.

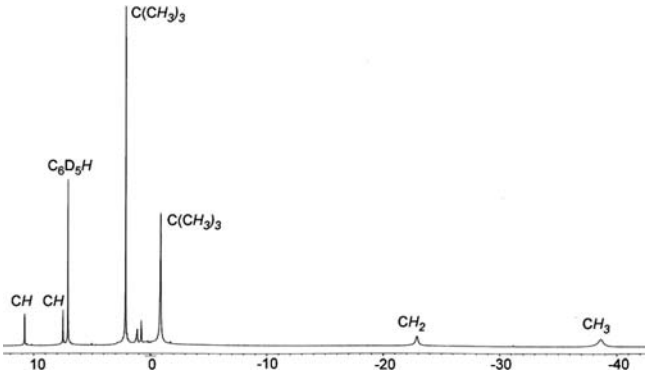

Figure 2. ^{1}H NMR spectrum of [(($^{t\,Bu}$ArO)$_3$mes)U] (**1-U**) in benzene-d$_6$.

Diffusion of pentane into a saturated toluene solution of **1-U** produced dark purple, rod-shaped crystals suitable for X-ray diffraction. The molecular structure, presented in Figure 3 (metrical parameters in Table 1), confirms the metalated product in crystals of [**1-U**·$^3/_4$ *n*-pentane·$^1/_4$ toluene] with an idealized C_3 symmetric molecule, where the uranium center is coordinated in a distorted trigonal pyramidal fashion to the three aryloxide groups. The average U−O bond distance of 2.16 Å is slightly shorter than what has been observed for the related [((^{R}ArO)$_3$tacn)U] system.[16] In accordance with its NMR spectrum, and in contrast to **2-U**, the aryloxide rings are positioned perpendicular to the arene and the plane formed by the three oxygen atoms. The uranium ion in **1-U** is located 0.46 Å below this plane toward the mesitylene. The mesitylene anchor is planar and interacts with the uranium in an η^6 fashion, with an average uranium−carbon bond distance of 2.73 Å (U−arene$_{cntr}$ = 2.33 Å), which is intermediate of previously reported uranium−arene compounds reported by Cummins and Ephritikhine.[11,19] The Cummins' system, with an activated arene ring, has an average U−C distance of 2.593(9) Å, corresponding to an average C−C distance of 1.438(13) Å. In contrast, the long U−C$_{avg}$ distance of 2.93(2) Å in Ephritikhine's arene compound, [(η^6-C$_6$Me$_6$)U(BH$_4$)$_3$],[19] indicates that the arene is weakly bound and not activated (C−C$_{avg}$ = 1.39(3) Å). The average C−C bond distance of the mesitylene ring in **1-U** (1.42 Å) is within error of that of the free ligand; thus, it seems there has been no significant reduction of the arene ring by the electron-rich uranium center. This observation is consistent with a uranium(III) ion coordinated to a neutral mesitylene anchor.

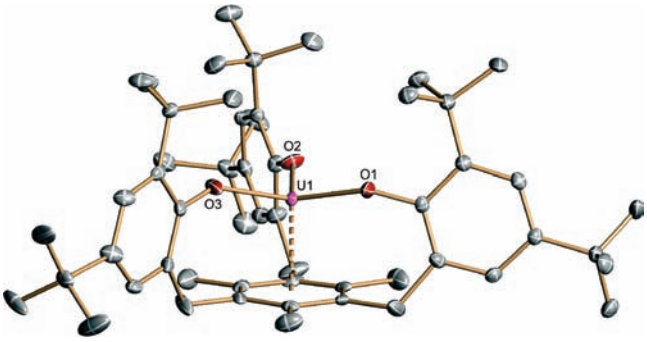

Figure 3. Molecular structure of [(($^{t\,Bu}$ArO$_3$)mes)U] (**1-U**) in crystals of (**1-U**·$^3/_4$ C$_5$H$_{12}$·$^1/_4$ CH$_3$C$_6$H$_5$). Hydrogen atoms and co-crystallized solvent molecules have been omitted for clarity.

Table 1. Selected Bond Distances (Å) for [(($^{t\,Bu}$ArO$_3$)mes)U](**1-U**)[a]

	distance (Å)		distance (Å)
U(1)−O(1)	2.167(2)	U(1)−C(6)	2.719(3)
U(1)−O(2)	2.158(2)	C(1)−C(2)	1.424(4)
U(1)−O(3)	2.166(2)	C(2)−C(3)	1.418(4)
U(1)−C(1)	2.745(3)	C(3)−C(4)	1.421(4)
U(1)−C(2)	2.740(3)	C(4)−C(5)	1.420(4)
U(1)−C(3)	2.722(3)	C(5)−C(6)	1.414(4)
U(1)−C(4)	2.737(3)	C(1)−C(6)	1.419(4)
U(1)−C(5)	2.723(3)	U$_{oop}$	−0.464(2)

[a] U$_{oop}$ is defined as the distance of the uranium ion below the plane of the three aryloxide oxygen atoms.

To further probe the electronic structure and oxidation state of **1-U**, a Kohn−Sham density functional theory (DFT) analysis and geometry optimization were performed with the ADF package,[20−22] employing the BP86 gradient corrected functional in the scalar zeroth−order regular approximation (ZORA).[23−27] Computed singly occupied molecular orbitals (SOMOs) and spin density for **1-U** are presented in Figure 4. The two lowest energy molecular orbitals, SOMO 1 and SOMO 2, feature δ backbonding interactions between the uranium f_{xyz} and $f_{z(x^2-y^2)}$ orbitals and the doubly degenerate π^* orbitals of the mesitylene ring. The SOMOs are composed of 5f uranium (70%) and empty π^* orbitals on the mesitylene ring (30%). The singly degenerate π^* orbital of φ character does not participate in the backbonding. The highest energy SOMO 3 is centered on uranium and is essentially nonbonding and mostly 5f uranium in character. The antibonding interactions with the oxygen atoms of the ligand are

(19) Baudry, D.; Bulot, E.; Charpin, P.; Ephritikhine, M.; Lance, M.; Nierlich, M.; Vigner, J. *J. Organomet. Chem.* **1989**, *371*, 155.

(20) te Velde, G.; Bickelhaupt, F. M.; van Gisbergen, S. J. A.; Fonseca Guerra, C.; Baerends, E. J.; Snijders, J. G.; Ziegler, T. *J. Comput. Chem.* **2001**, *22*, 931.

(21) Fonseca Guerra, C.; Snijders, J. G.; te Velde, G.; Baerends, E. J. *Theor. Chem. Acc.* **1998**, *99*, 391.

(22) *ADF2007.01, S.*; Theoretical Chemistry, Vrije Universiteit: Amsterdam, The Netherlands, http://www.scm.com.

(23) Van Lenthe, E.; Baerends, E. J.; Snijders, J. G. *J. Chem. Phys.* **1993**, *99*, 4597.

(24) Van Lenthe, E.; Baerends, E. J.; Snijders, J. G. *J. Chem. Phys.* **1994**, *101*(11), 9783.

(25) Van Lenthe, E.; Ehlers, A. E.; Baerends, E. J. *J. Chem. Phys.* **1999**, *110*, 8943.

(26) Perdew, J. P. *Phys. Rev. B* **1986**, *33*(12), 8822.

(27) Becke, A. D. *Phys. Rev. A* **1988**, *38*, 3098.

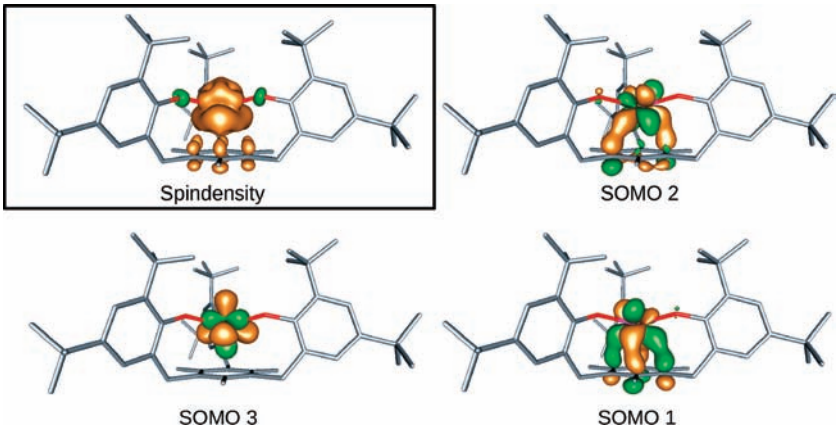

Figure 4. Computed SOMOs and spin density plot of [(($^{t\,Bu}$ArO)$_3$mes)U] (**1-U**).[23]

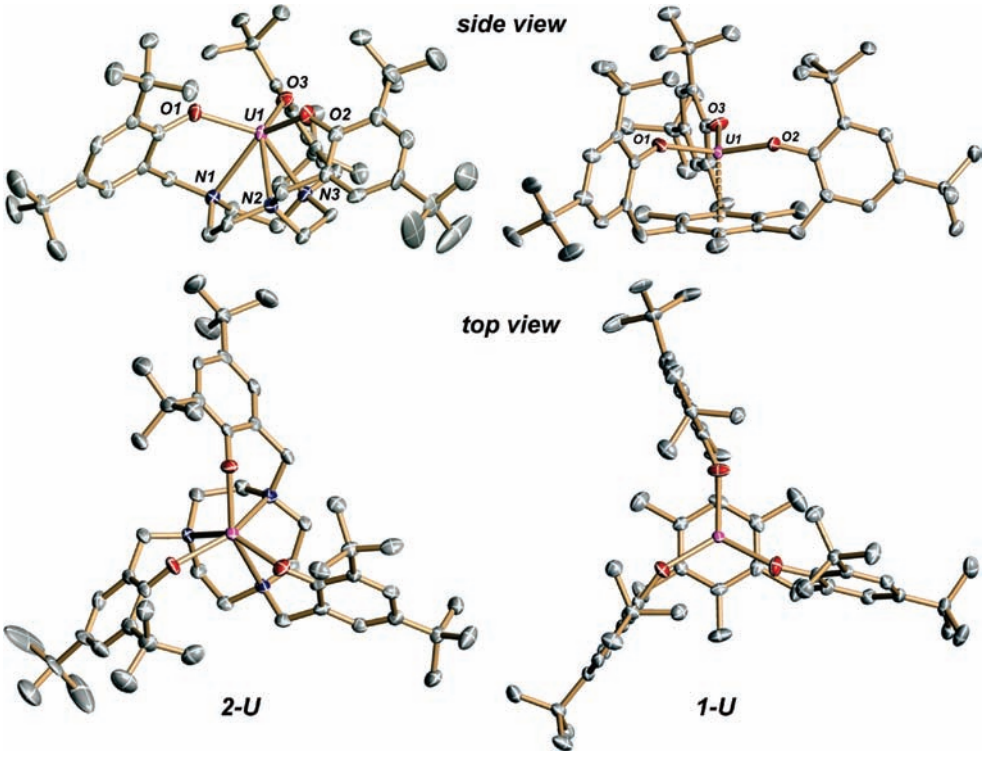

Figure 5. Comparison of the molecular structures from the side view (top) and top view (bottom) of [(($^{t\,Bu}$ArO)$_3$tacn)U] (**2-U**) and [(($^{t\,Bu}$ArO)$_3$mes)U] (**1-U**). Hydrogen atoms and solvent molecules have been omitted for clarity.

reduced by mixing in approximately 14% of the empty uranium 7s orbital, thereby effectively lowering the energy of this SOMO 3. The majority of the spin is located on the uranium center, which has a Mulliken spin density of 2.72 (to be compared with 3.11 found for [((ArO)$_3$tacn)U^{III}]). The remaining 15% of the α spin is found on the mesitylene carbons. The DFT analysis thus corroborates the assignment of **1-U** as a uranium(III) f^3 complex.

A comparison of the molecular structure of the uranium(III) complex **1-U** to the previously synthesized uranium(III) complex, [(($^{t\,Bu}$ArO)$_3$tacn)U] (**2-U**), bearing the aryloxide functionalized triazacyclononane ligand, is presented in Figure 5. Both complexes, **1-U** and **2-U**, have *tert*-butyl substituents on the aryloxide rings that surround and protect the uranium center, while the mesitylene anchor of **1-U** and the triazacyclononane fragment of **2-U** protect one side of the uranium ions from undesired reactions. The side views of both molecules show one open coordination site above each uranium center for small molecule coordination, and possibly, activation events. The main difference can be observed by examining the top view of both molecules. It is evident that the aryloxide groups in **2-U** are not perpendicular to the triazacyclononane plane but rather oriented in a propeller-like fashion, whereas the *tert*-butyl groups in **1-U** are arranged nearly perpendicular to the arene anchor. As a result, the *tert*-butyl substituents in **2-U** are less protective of the uranium center compared to **1-U**. This is illustrated by the relative reactivity of the two complexes, and explains the propensity of [(($^{t\,Bu}$ArO)$_3$tacn)U] (**2-U**) to form the uranium(IV) μ-oxo dimer, [{(($^{t\,Bu}$ArO)$_3$tacn)U}$_2$(μ-O)], upon exposure to ethers.[17] On the other hand, complex **1-U** is considerably more stable to diethyl ether and does not undergo rapid oxygen abstraction even after days of exposure.

Scheme 2. Synthesis of [(($^{t\,Bu}$ArO$_3$)mes)U(dbabh)] (**1-Udbabh**) and [(($^{t\,Bu}$ArO$_3$)tacn)U(dbabh)] (**2-Udbabh**)

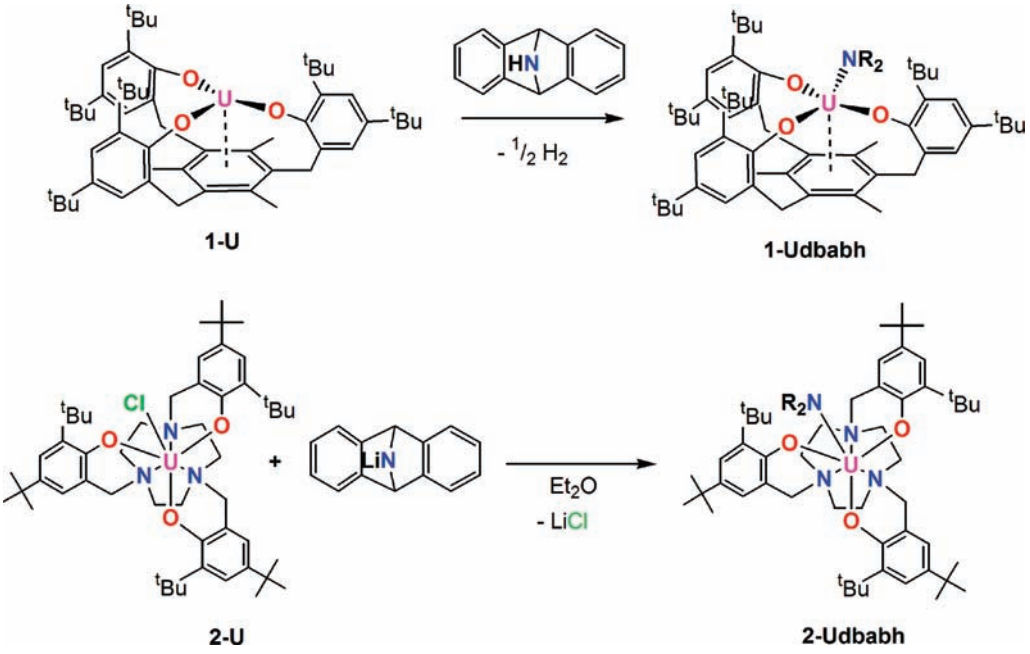

The reactivity of **1-U** was tested with the sterically hindered amine, Hdbabh[28] (2,3:5,6-dibenzo-7-azabicyclo[2.2.1]hepta-2,5-diene, Scheme 2). Treating a dark purple solution of **1-U** with 1 equiv of Hdbabh produced a bright orange solution. Analysis of the resulting orange products by ^{1}H NMR spectroscopy revealed a paramagnetically broadened and shifted spectrum, with the two *tert*-butyl resonances for the ligand appearing at 10.96 and 5.65 ppm. The resonance for the methyl groups on the mesitylene anchor was shifted to −22.19 ppm from −38.61 ppm in the uranium(III) starting material. The assignment of additional paramagnetically broadened and shifted signals remains equivocal; however, their presence is indicative of deviation from idealized C_3 symmetry as observed in precursor complex **1-U**.

Single crystals suitable for X-ray crystallography were obtained by cooling a concentrated solution of the orange product in pentane to −35 °C. The molecular structure reveals the uranium(IV) amide species, [(($^{t\,Bu}$ArO)$_3$mes)U(dbabh)] (**1-Udbabh**), resulting from N−H activation of the amine and elimination of hydrogen (Figure 6, middle).[30a] The average uranium−oxygen distance is 2.16 Å, while the U−C distances are the same within error and have an average value of 2.88 Å. The U−N distance of 2.247(4) Å is consistent with other crystallographically characterized uranium−dbabh amide species, such as in [U(dbabh)$_6$] and its one-electron reduced anion.[28] The most notable feature of this structure is that the amide ligand is not located along the idealized C_3 axis of the ligand as expected and consistently observed in seven-coordinate complexes of [(($^{t\,Bu}$ArO$_3$)tacn)U(L)] (L = axial ligand). Instead, the aryloxide oxygen atoms O(1) and O(3) have shifted substantially from ∠(O−U−O) of 113.59(8)° in the starting material to 168.07(12)° in **1-Udbabh**, consequently allowing the amide substituent to be nearly coplanar with these ligand arms.

To deduce whether this unusual arrangement is due to steric or electronic effects of the new ligand system, synthesis of the same uranium amido derivative was attempted with the tacn ligand system via the same procedure as **1-Udbabh**. In contrast to **1-U**, addition of the neutral amine to **2-U** did not result in the desired N−H activation to form the uranium amide. Instead, no color change or reaction occurred, and as a result, the synthesis was attempted using a salt metathesis route (Scheme 2). Addition of Lidbabh·Et$_2$O to the uranium(IV) chloro complex, [(($^{t\,Bu}$ArO)$_3$tacn)UCl)] (see Supporting Information), in ether followed by stirring overnight resulted in a color change from pale green to dark yellow. Removal of the ether in vacuo followed by filtration with hexane over Celite to remove the lithium chloride provided a yellow solution, which, when cooled, resulted in the precipitation of yellow microcrystals. The observed reactivity illustrates the flexibility of the mesitylene-anchored ligand, as it can move to allow the bulky neutral amine to access the uranium center *cis* to the arene. This is in contrast to the more rigid triazacyclononane-anchored ligand, which limits, because of propeller-type arrangement of the aryloxide, side access to the uranium center.

Crystals of the **2-U** amido species were grown by cooling a concentrated hexane solution of the yellow product to −35 °C in the glovebox freezer. Analysis of the yellow blocks revealed the seven coordinate uranium dbabh amido complex, [(($^{t\,Bu}$ArO)$_3$tacn)U(dbabh)] (**2-Udbabh**), which features the amido ligand coordinated along the idealized C_3 axis (Figure 6, top). The uranium-ligand distances were as expected, with respective U−O$_{avg}$ and U−N$_{avg}$ distances of 2.21 and 2.72 Å. The U−N(dbabh) distance of 2.260(5) is similar to that of the mesitylene based analogue, [(($^{t\,Bu}$ArO)$_3$mes)U(dbabh)] (Table 2). The O(2)−U(1)−N(dbabh) angle in **2-Udbabh**, however, is 83.46(17)°, showing that this substituent is close to perpendicular (90°) with the trigonal plane formed by the aryloxide oxygens of the ligand. In contrast, the same angle for the mesitylene anchored system is 142.33(14)°, which deviates significantly from a perpendicular arrangement.

The newly found coordination geometry for uranium complexes with mesitylene-anchored aryloxides is most likely a consequence of both steric and electronic effects imposed by the arene anchor. First, the mesitylene-based ligand system

(28) Meyer, K.; Mindiola, D. J.; Baker, T. A.; Davis, W. M.; Cummins, C. C. *Angew. Chem., Int. Ed.* **2000**, *39*, 3063.

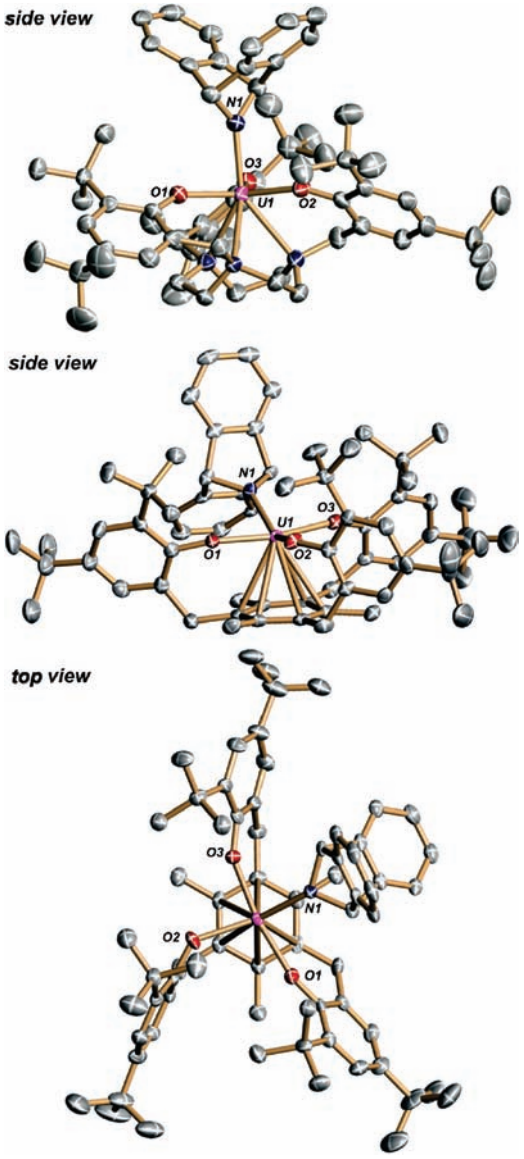

Figure 6. Comparison of the molecular structures from the side view and top view of [(($^{t\,Bu}$ArO)$_3$mes)U(dbabh)] (**1-Udbabh**) in crystals of (**1-Udbabh**·$^1/_2$C$_{14}$H$_{10}$·C$_5$H$_{12}$) (middle and bottom) and [(($^{t\,Bu}$ArO)$_3$tacn)U(dbabh)] (**2-Udbabh**) in crystals of (**2-Udbabh**·2 C$_5$H$_{12}$) (top). Hydrogen atoms and co-crystallized solvent molecules have been omitted for clarity.

leads to a flexible picket fence-type arrangement of the aryloxide ligands, thereby allowing for better side-on access of Hdbabh to the uranium ion as compared to the propeller-type arrangement preferred in the triazacyclononane-based ligand system. The perpendicular arrangement of three *tert*-butyl groups in **1-U** may interfere sterically with a bulky, axially oriented dbabh amide ligand.

It also is suggested that the δ-backbonding interaction in the mesitylene-anchored uranium complex depletes electron density from the reactive site *trans* to the arene, thus directing the seventh ligand away from linear axial binding. Hence, coordination in the plane with the three aryloxide groups may be beneficial because of better metal−ligand orbital overlap.

In contrast, the cyclic triazacyclononane fragment is not a strong ligand for U(III) and U(IV) ions and does not involve the uranium orbitals to the same extent. Accordingly, ligand binding and substrate activation events are directed *trans* to the triazacyclononane anchor, perpendicular to the tris-aryloxide plane. The reaction with Hdbabh shows that the mesitylene anchor of **1-Udbabh** greatly influences the reactivity by introducing different steric and electronic effects to the resulting U(III) precursor. The unusual binding mode of the dbabh amide in **1-Udbabh** is a direct consequence of new electronic properties introduced by the mesitylene anchor, which do not exist in the redox-innocent tacn ligand framework of **2-Udbabh**.

Table 2. Selected Bond Distances (Å) for **1-Udbabh** and **2-Udbabh**

	1-Udbabh	**2-Udbabh**
U(1)−O(1)	2.138(3)	2.220(4)
U(1)−O(2)	2.182(3)	2.212(4)
U(1)−O(3)	2.158(3)	2.203(4)
U−Oavg	2.16	2.21
U(1)−C(1)	2.872(5)	
U(1)−C(2)	2.879(5)	
U(1)−C(3)	2.869(5)	
U(1)−C(4)	2.912(5)	
U(1)−C(5)	2.940(5)	
U(1)−C(6)	2.852(5)	
C(1)−C(2)	1.414(7)	
C(2)−C(3)	1.424(7)	
C(3)−C(4)	1.414(7)	
C(4)−C(5)	1.405(7)	
C(5)−C(6)	1.420(7)	
C(1)−C(6)	1.418(7)	
U(1)−N(1)		2.714(5)
U(1)−N(2)		2.688(5)
U(1)−N(3)		2.752(5)
U−Navg		2.72
U(1)−N(dbabh)	2.247(4)	2.260(5)

In addition to X-ray crystallography, NMR spectroscopy, and combustion analyses, complexes **1-U**, **1-Udbabh**, and **2-Udbabh** were characterized by SQUID magnetometry (Figure 7) and electronic absorption spectroscopy (Figure 8) under strictly air-free conditions. Variable temperature SQUID magnetization data often provide information on oxidation state and other electronic properties of the complex. The variable temperature SQUID spectrum of **1-U** displays a magnetic moment of 1.15 μ_B at 5 K, increasing to 1.92 μ_B at 300 K. These highly reproducible values are remarkably low compared to those observed for trivalent complexes of [((^{R}ArO)$_3$tacn)U], which range from 1.66 μ_B at 4 K to 2.90 μ_B at 300 K (R = ^{t}Bu) and 1.74 μ_B at 5 K to 2.83 μ_B at 300 K (R = Ad).[16,29] Interestingly, the magnetization data for trivalent **1-U** are more reminiscent of data obtained for imido and oxo U(V) f^1 complexes [((ArO)$_3$tacn)U(L)] (L = RN^{2-}, O^{2-}; R = 2,4,6-trimethylphenyl), which range from 1.55 at 5 K to 1.98 μ_B at room temperature.[30a] Although intriguing, a formulation of **1-U** being a formally pentavalent species with a doubly reduced arene ligand is not supported by the above presented reactivity, structural, and computational study. It should be noted, however, that the temperature dependency of the magnetic moment of trivalent **1-U** (f^3) is significantly lower than those typically observed for U(IV) f^2 amide complexes of the [((^{R}ArO)$_3$tacn)U][30a] as well as the newly developed [((^{R}ArO)$_3$mes)U] system (vide infra). Increased covalency through δ-backbonding interaction observed for **1-U** (vide supra) may be responsible for lowering the magnetic moment by quenching the orbital angular contribution to the magnetic moment.[30b]

(29) Nakai, H.; Hu, X.; Zakharov, L. N.; Rheingold, A. L.; Meyer, K. *Inorg. Chem.* **2004**, *43*, 855.

(30) (a) Bart, S. C.; Anthon, C.; Heinemann, F. W.; Bill, E.; Edelstein, N. M.; Meyer, K. *J. Am. Chem. Soc.* **2008**, *130*, 12536. (b) Siddall, T. H., III In *Theory and Applications of Molecular Paramagnetism*; Boudreaux, E. A., Mulay, L. N., Eds.; John Wiley and Sons: New York, 1976.

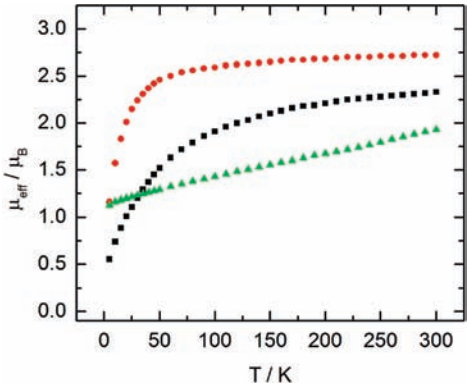

Figure 7. Temperature-dependent SQUID magnetization data (at 1 T) for microcrystalline samples of **1-U** (green triangles), **1-Udbabh** (black squares), and **2-Udbabh** (red circles) plotted as a function of magnetic moment (μ_{eff}) vs temperature (T). Data were corrected for underlying diamagnetism, and reproducibility was checked on multiple independently synthesized samples of each (see Supporting Information).

The variable temperature magnetic behavior of both U(IV) complexes, **1-Udbabh** and **2-Udbabh**, was studied over the same temperature range (5−300 K, Figure 7). As expected for tetravalent uranium complexes, the magnetic moment exhibits strong temperature dependence, with values ranging from 2.37 μ_B at 300 K that decrease steadily to 0.54 μ_B at 5 K (Figure 5) for **1-Udbabh**.[31] Despite the highly unusual data obtained for the U(III) precursor, **1-U**, the magnetic data for U(IV) amide **1-Udbabh** are less surprising, albeit still slightly lower than the analogous compound **2-Udbabh** with magnetic moment values ranging from 2.72 μ_B at 300 K to 1.16 μ_B at 5 K. This phenomenon is consistent with a weakly interacting triazacyclononane anchor of **2-Udbabh** resulting in reduction of the quenching effects that lower the magnetic moment. The reduction of magnetic moment at low temperature is consistent with a poorly isolated singlet ground state arising from crystal field effects, which can occur in U(IV) complexes.[32]

The unusual electronic structure of **1-U**, suggested by the magnetization data, is also reflected in its UV/vis/NIR electronic absorption spectrum, which exhibits distinctly different absorption features compared to U(III) complexes of the [((^{R}ArO)$_3$tacn)U] system. The absorption spectrum of purple **1-U** (Figure 8, top), recorded in toluene (300−2100 nm) at ambient temperature, reveals low- to mid-intensity absorption bands in the range of 400−1600 nm. The color giving band at 498 nm (ε = 1306 M^{-1} cm^{-1}), can be assigned to the Laporte-allowed $5f^3$ to $5f^26d^1$ transition, which is observed at 460 nm (ε = 2340 M^{-1} cm^{-1}) and 424 nm (ε = 1945 M^{-1} cm^{-1}), respectively, in [((^{R}ArO)$_3$tacn)U] with R = ^{t}Bu and Ad. Another mid-intensity feature, previously not observed in complexes of U(III), is centered at 700 nm ($\varepsilon \approx$ 645 M^{-1} cm^{-1}), and could be assigned to a charge-transfer band, possibly from occupied δ-type U orbitals to the arene's empty π^* orbitals. Additionally, weaker f−f absorption bands are spread over the entire UV/vis and NIR region of the spectrum. It is notable, however, that these bands are considerably broader and more intense than the f−f absorption bands observed in spectra of **2-U**, consistent with a higher degree of covalency in **1-U**. Thus, using the mesitylene anchor in the ligand framework changes

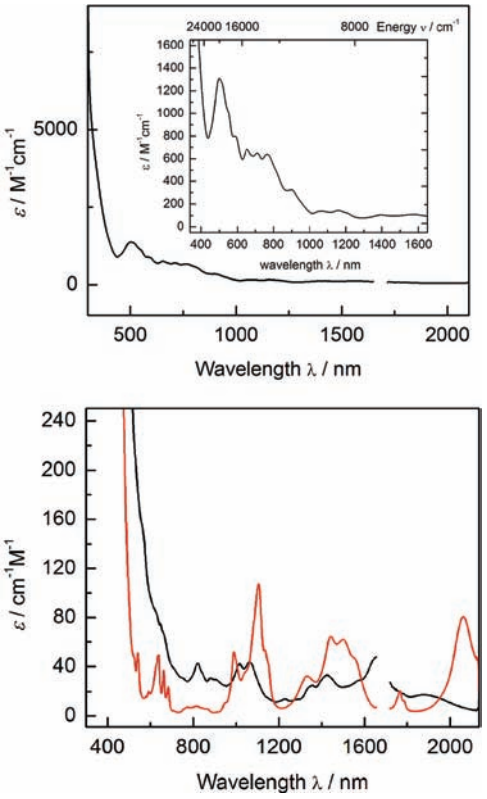

Figure 8. Electronic absorption spectra of **1-U** (top), **2-Udbabh** (red, bottom), and **1-Udbabh** (black, bottom), all recorded in toluene.

the complexes' electronic structure markedly, and hence, differences in reactivity are to be expected.

In contrast, the mesitylene-based uranium(IV) complexes display the expected UV/vis/NIR electronic absorption spectra as measured from 300−2100 nm (Figure 8, bottom). Analysis of a toluene solution of **1-Udbabh** shows a charge transfer band at 431 nm ($\varepsilon \approx$ 1016 M^{-1} cm^{-1}), responsible for the orange color, in addition to weak f−f transitions from 500−2100 (ε = 14−85 M^{-1} cm^{-1}, Figure 8, bottom). The triazacyclononane derivative **2-Udbabh** exhibits similar sharp, yet weakly intense (ε = 10−108 M^{-1} cm^{-1}) f−f transitions over the same range. Additionally, a band observed at 408 nm (ε = 1943 M^{-1} cm^{-1}) is responsible for the complexes' intense yellow color. The electronic absorption spectra displayed here demonstrate a similar trend as observed for the previously presented magnetic data for the arene based ligand system, in that the uranium(III) complex, **1-U**, has an unusual characteristic spectrum, whereas that of the uranium(IV) amide is unexceptional.

Conclusions

The studies presented here demonstrate that a change in a ligand framework, such as the substitution of the anchor group, can significantly alter the electronic properties and reactivity of the compound. The new tripodal ligand system presented can be readily synthesized and modified both electronically and sterically. Accordingly, changing either the substituents on the arene anchor or those on the aryloxide rings creates a highly modular new ligand system.

Crystallographic characterization of the low-valent U(III) complex reveals an η^6-binding mode of the mesitylene anchor

(31) Castro-Rodriguez, I.; Meyer, K. *Chem. Commun.* **2006**, 1353.
(32) Stewart, J. L.; Andersen, R. A. *New J. Chem.* **1995**, *19*, 587.
(33) Stewart, J. L.; Andersen, R. A. *Polyhedron* **1998**, *17*, 953.

to the uranium ion. Theoretical calculations confirm a covalent δ bonding interaction in accord with unusual magnetic and spectroscopic features. The striking differences in the electronic structure of the trivalent mesityl-anchored complex **1-U**, when compared to the triazacyclononane-based **2-U**, are manifested in the magnetic moment and electronic absorption spectra. The uranium f to mesityl π^* δ-interaction present in **1-U** and absent in **2-U** is most likely the origin of this difference. A structural comparison to the well established U(III) complex, [(($^{t\,Bu}$ArO)$_3$tacn)U], bearing the triazacyclononane anchor, demonstrates that the uranium center in **1-U** is more protected from access along the C_3, and consequently, directs Hdbabh *cis* to the arene anchor. As a result, the uranium(IV) amide derivatives of both ligand sets display an interesting structural dichotomy, in that the triazacyclononane ligand orients the amide substituent, as all other seventh ligands tested so far, along the C_3 axis, whereas in the mesitylene anchored ligand system, the same incoming bulky amide ligand is placed closer to the trigonal tris-aryloxide plane. These uranium(IV) derivatives highlight the greater flexibility of the new ligand system, indicating that this highly modular ligand will be a promising candidate for supporting metal centers of a various range of sizes and oxidation states.

Further studies will focus on the exploration of the potential redox-activity of this ligand system for the discovery of unusual reactivity, such as the reductive activation of otherwise unreactive small molecules.

Experimental Section

Preparation of Ligand (1). This synthesis was adapted from a literature procedure.[3] A 500 mL Schlenk flask was charged with 5.00 g (18.7 mmol) of tris(chloromethyl) mesitylene), 11.70 g (56.8 mmol) of 2,4-di-*tert*-butyl phenol, and 8 g (59 mmol) of $ZnCl_2$. Dry chloroform was added, and the solution refluxed for 2 days under nitrogen. The solution was cooled to room temperature, washed with saturated ammonium chloride, and the organics separated and dried over $MgSO_4$. The volatiles were removed by rotary evaporation. The resultant residue (yellow oil) was dissolved in a minimal amount of hexane to make a saturated solution. Cooling in the freezer resulted in a white precipitate, which was isolated by filtration and washed with cold hexane. The filtrate was concentrated and more ligand was collected. Yield: 6.5 g (48%). Elemental Analysis for $C_{54}H_{78}O_3$: Calcd: C, 83.67, H, 10.14; Found C, 83.43, H,10.17. ^{1}H NMR (C_6D_6): δ (ppm) = 1.09 (s, 27H, ^{t}Bu), 1.34 (s, 27H, ^{t}Bu), 2.10 (s, 9H, CH_3), 3.94 (s, 6H, CH_2), 4.87 (bs, 1H, OH), 6.63 (d, J = 2.34, 3H, CH (aryl)), 7.07 (d, J = 2.34, 3H, CH (aryl)).^{13}C NMR ($CDCl_3$): δ (ppm) = 17.05 (3C, Mes*C*H3), 30.01 (o-C*C*H3), 31.70 (p-C*C*H3), 31.84 (mesC*C*H2), 34.20 ((p-*C*CH3), 34.69 ((o-*C*CH3), 121.64 (o-*C*), 123.24 (pC*C*o-C), 124.58 (m-C), 134.12 (mes*C*CH2), 134.76 (o-*C*), 136.18 (Mes*C*-(CH3), 142.16 (p*C*CCH3), 150.46 (*C*OH).

Preparation of [((^{t}BuArO)$_3$mes)U] (1-U). In the glovebox, a 100 mL round-bottom flask was charged with 0.666 g (0.86 mmol) of **1**. Approximately 100 mL of pentane was added to dissolve the ligand. A vial was charged with 0.672 g (0.86 mmol) of [U(N(SiMe$_3$)$_2$)$_3$] and dissolved in approximately 20 mL of pentane. The [U(N(SiMe$_3$)$_2$)$_3$] solution was added to the round-bottom flask while stirring. This was stirred overnight, followed by filtration over a pad of Celite and removal of the volatiles to leave 0.543 g (63%) of a purple solid. Elemental Analysis for $C_{54}H_{75}O_3U$: Calcd: C, 64.01, H, 7.76; Found C, 63.67, H, 7.50. ^{1}H NMR (C_6D_6): δ (ppm) = −38.61 (s, 26.80, 9H, CH_3), −22.87 (s, 34.14, 6H, CH_2), −0.85 (s, 18.64, 27H, ^{t}Bu), 2.03 (s, 3.84, 27H, ^{t}Bu), 7.58 (s, 6.58, 3H, CH (aryl)), 10.66 (s, 6.59, 3H, CH (aryl)).

Preparation of [((^{t}BuArO)$_3$mes)U(dbabh)] (1-Udbabh). A 20 mL scintillation vial was charged with 0.150 g (0.148 mmol) of **1-U** and approximately 5 mL of toluene. One equivalent, 0.028 g (0.148 mmol) of Hdbabh was weighed into a separate vial, dissolved in 2−3 mL more of toluene, and slowly added to the solution. This was stirred overnight, and changed color from dark purple to bright orange. After this time, the toluene was removed in vacuo. The residue was dissolved in pentane and filtered over Celite. Removal of the volatiles in vacuo produced an orange powder, which was recrystallized from pentane to produce 0.103 g of an orange solid (58%). Elemental Analysis for $C_{68}H_{85}O_3NU$: Calcd: C, 67.92, H, 7.13, N, 1.16; Found C, 68.74, H, 7.04, N, 1.19. ^{1}H NMR (C_6D_6): δ (ppm) = −33.45 (s, 6.56, 3H), −22.19 (s, 5.85, 9H, CH_3), −10.83 (d, 16.5 Hz, 2H, C*H* (dbabh)), −8.00 (d, 16.5 Hz, 2H, C*H* (dbabh)), −6.00 (s, 7.62, 2H), 1.94(s, 4.59, 6H), 2.44 (s, 7.56, 3H, CH_3), 3.66 (s, 16.62, 2H), 5.65 (s, 5.15, 27H, C(CH_3)$_3$), 6.42 (s, 32.58, 3H), 10.96 (s, 6.71, 27H, C(CH_3)$_3$), 14.47 (s, 7.39, 2H), 22.12 (s, 7.31, 2H), 26.92 (s, 9.13, 2H).

Preparation of [((^{t}BuArO$_3$)tacn)UCl] (2-UCl). A 20 mL scintillation vial was charged with 0.160 g (0.157 mmol) of [(($^{t\,Bu}$ArO$_3$)tacn)U] and approximately 10 mL of pentane. While stirring, several drops of methylene chloride were added to the dark red solution until the color changed to pale green and a precipitate formed. After stirring the solution for approximately 3 h, all of the volatiles were removed in vacuo, and pentane was added to the residue, which was stirred vigorously. The precipitate was isolated by vacuum filtration with a fritted filter funnel and dried thoroughly to produce 0.148 g (0.140 mmol, 89%) of "[(($^{t\,Bu}$ArO$_3$)tacn)UCl]". A molecular structure of this complex was not obtained, but NMR evidence supports the formation of a bridged dimer, [(($^{t\,Bu}$ArO$_3$)tacn)UCl]$_2$, with a U_2Cl_2 diamond core structure. Elemental Analysis for $C_{51}H_{78}O_3N_3UCl$: Calcd: C, 58.08, H, 7.45, N, 3.98; Found C, 57.78, H, 7.45, N, 4.18. ^{1}H NMR (CD_2Cl_2): δ (ppm) = −79.98 (14.48, 3H, CH_2), −10.38 (39.41, 3H, CH_2), −6.94 (15.67, 18H, C(CH_3)$_3$), −6.28 (16.50, 4H), −2.95 (43.82, 6H), −2.17 (13.07, 18H, C-(CH_3)$_3$), −0.56 (21.86, 4H), 1.74 (13.31, 36H, C(CH_3)$_3$)), 2.54 (15.39, 36H, C(CH_3)$_3$), 4.95 (26.97, 4H), 7.55 (14.94, 6H), 10.46 (14.90, 6H), 29.59 (26.64, 6H), 31.95 (39.58, 6H), 65.68 (10.01, 3H).

Preparation of [((^{t}BuArO$_3$)tacn)U(dbabh)] (2-Udbabh). A 20 mL scintillation vial was charged with 0.070 g (0.066 mmol) of [(($^{t\,Bu}$ArO$_3$)tacn)UCl] and approximately 5 mL of ether. In a separate vial, 0.017 g (0.066 mmol) of Lidbabh·Et$_2$O was weighed and dissolved in 5 mL of ether. While stirring, the Lidbabh solution was added to the light green solution of [(($^{t\,Bu}$ArO$_3$)tacn)UCl], and this was stirred for 16 h. After this time, the ether was removed in vacuo, and the residue extracted with hexane. The hexane mixture was filtered over Celite, and removal of the solvent in vacuo produced 0.063 g (0.052 mmol, 78%) of [(($^{t\,Bu}$ArO$_3$)tacn)U(dbabh)]. Elemental Analysis for $C_{65}H_{88}O_3N_4U$: Calcd: C, 64.44, H, 7.32, N, 4.62; Found C, 65.13, H, 7.28, N, 4.69. ^{1}H NMR (C_6D_6): δ (ppm) = −119.62 (52.30, 3H, CH_2), −16.39 (23.40, 27H, C(CH_3)$_3$), −11.12 (35.44, 3H, CH_2), −5.43 (23.98, 3H), −4.62 (24.81, 3H), −3.67 (23.03, 27H, C(CH_3)$_3$), 18.78 (29.44, 4H, C*H* of dbabh), 29.10 (d, 4H, C*H* of dbabh), 45.03 (36.89, 2H), 46.10 (37.39, 2H), 90.23 (36.39, 2H), 96.04 (43.87, 4H).

Acknowledgment. The Deutsche Forschungsgemeinschaft and Sonderforschungsbereich 583 are acknowledged for financial support. S.C.B. is grateful for an Alexander von Humboldt Postdoctoral Fellowship.

Supporting Information Available: General considerations, NMR data, and crystallographic techniques and tables. This material is available free of charge via the Internet at http://pubs.acs.org.